Integrating electromagnetic induction measurements and electrical resistivity tomography to monitor rainwater lenses in Dutch polders

Carrizo, M.; Riakhi, F.; Slob, E.; Werthmüller, D.; van Breukelen, B.

DOI
10.3997/2214-4609.202420119

Publication date
2024

Document Version
Final published version

Citation (APA)
Carrizo, M., Riakhi, F., Slob, E., Werthmüller, D., & van Breukelen, B. (2024). *Integrating electromagnetic induction measurements and electrical resistivity tomography to monitor rainwater lenses in Dutch polders*. Paper presented at Near Surface Geoscience 2024, Helsinki, Finland. https://doi.org/10.3997/2214-4609.202420119

EAGE

CONFERENCE & EXHIBITION
NEAR SURFACE GEOSCIENCE'24

Integrating electromagnetic induction measurements and electrical resistivity tomography to monitor rainwater lenses in Dutch polders

M. Carrizo[1], F. Riakhi[2], E. Slob[1], D. Werthmüller[1], B. Van Breukelen[2]

[1] Delft University of Technology, Faculty of Civil Engineering and Geosciences, Department of Geosciences and Engineering; [2] Delft University of Technology, Faculty of Civil Engineering and Geosciences, Department of Water Management

Summary

In agriculture, there is a demand for new methods to monitor the dynamics of fresh rainwater lenses overlaying on saline seeping groundwater. For this purpose, integrating different geoelectrical measurements is a non-invasive and low-cost approach to obtaining subsurface information. Geoelectric methods such as electromagnetic induction (EMI) and electrical resistivity tomography (ERT) have proven effective in characterizing subsoil electrical properties, which can be correlated to petrophysical properties such as fluid salinity. These methods have different sensitivities and can provide complementary information about the electrical conductivity and geometry of the subsurface. This study explores the effectiveness of a methodology that combines EMI measurements with laterally constrained inversion as prior information for ERT inversion. We investigate the usefulness of the method using synthetic data and data from a coastal Dutch polder system. The findings are promising, demonstrating improved delineation of changes in electrical conductivity, potentially linked with salinity fluctuations in the subsoil. This methodology proves effective in mapping in-depth variations in electrical conductivity. It could facilitate the impact assessment of level-controlled drainage systems on augmenting shallow rainwater lenses and mitigating salinization in Dutch polders.

Integrating electromagnetic induction measurements and electrical resistivity tomography to monitor rainwater lenses in Dutch polders.

Introduction

The basic Electromagnetic Induction (EMI) instrument consists of a transmitter coil and a receiver coil. An alternating current flowing in the transmitter coil generates a primary electromagnetic field. According to Faraday's law, an oscillating primary electromagnetic field creates eddy currents in conductive bodies. These eddy currents induce a secondary electromagnetic field, which can be measured by the receiver loop at the surface. The primary and secondary electromagnetic field fluxes go through the receiver coil inducing a voltage measured by the instrument. This measurement can provide information about the subsurface geometry and geoelectrical properties (Kearey et al., 2002). Apart from the subsurface conductivity, the strength of the secondary electromagnetic field depends on the transmitter-receiver coil configuration and the operating frequency. The measured electromagnetic field is a complex quantity expressed as in-phase (real part) and quadrature (imaginary part) components.

EMI instruments are commonly used to estimate the electrical conductivity of the shallow subsurface for hydrogeological studies (Paz et al., 2024; Paepen et al., 2020). The EMI measurements are useful for mapping variations related to the petrophysical properties of the water contained in the soil, such as salinity. A common method to invert this data is the laterally constrained inversion (LCI) proposed by Auken and Christiansen (2004), used previously in EMI inversion (Klose et al., 2022; Thalhammer, 2022). The inversion of geoelectric methods can be carried out separately or jointly, allowing interpreters to derive a conceptual model that validates the changes in the geology as well as other physical properties (Paz et al., 2024; Paepen et al., 2020). In this study, we investigate the integration of EMI and Electrical Resistivity Tomography (ERT) methods. Both measure the electrical conductivity of the subsurface, however, they have different sensitivities. The EMI method is more sensitive to conductive bodies but can have problems resolving resistive zones, whereas the ERT method can image conductive and resistive variations. Moreover, the EMI method is less expensive and easier to collect the data, which seems a great way to provide additional information. The exploration depth in both methods differs but they can complement each other.

Within the Dutch polders, groundwater has become brackish or saline due to seawater intrusion and marine transgressions (Stofberg et al., 2017). This saline groundwater flows upward, driven by a regional hydraulic gradient to the surface, thereby obstructing deeper infiltration of fresh rainwater. This results in the formation of thin and shallow rainwater lenses (RWLs), which take a buoyant and lenticular shape atop saline groundwater (Louw et al., 2013). To combat the salinization issue in these deltaic areas, level-controlled drainage (LCD) is designed to enhance the thickness of these RWLs during the autumn and winter. This is achieved by storing fresh rainwater in the soil and preserving any surplus that is pretreated in the underlying aquifer using the Aquifer Storage and Recovery (ASR) technique. During the crop-growing season, from spring to summer, the same subsurface drainage system is utilized for sub-irrigation using ASR water as an external water supply. We investigate the potential of using an integrated approach for EMI LCI and ERT inversion to map fresh-saline groundwater dynamics. Our study includes a synthetic example and a case study in a coastal Dutch polder system.

Methodology

We carry out the EMI inversion using the LCI method. An LCI produces a simultaneous inversion of adjacent sounding locations to obtain quasi-layered subsurface models. As first introduced by Auken and Christiansen (2004), the 1D-LCI scheme produces pseudo-2D models from 1D soundings using a set of laterally constrained calculations. The basic assumption of the LCI concept is that the lateral constraints are considered prior information on the spatial variability in the area. Lateral continuity is imposed by regularizing the inverse problem by constraining neighboring model parameters (Auken and Christiansen, 2004). The objective function is expressed as:

$$\Phi_{\mathbf{m}} = \|\mathbf{W}_{\mathrm{D}}(f(\mathbf{m}) - \mathbf{d})\|_2^2 + \lambda \|\mathbf{R}\mathbf{C}_{\mathrm{R}}(\mathbf{m} - \mathbf{m}_{\mathrm{ref}})\|_2^2 \rightarrow min, \quad (1)$$

Table 1 *Instruments configuration for simulation and acquisition*

EMI Survey	ERT survey
Coil geometry: HCP, PRP HCP offsets: 2m, 4m, 8m. PRP offsets: 2.1m, 4.1, 8.1m Frequency: 9000 Hz, Height: 0.1m	Array configuration: Dipole - Dipole 72 electrodes Start: 0m, End: 36m, Spacing: 0.5m

where $\mathbf{W}_\mathrm{D}$ represents the data weighting matrix, $\mathbf{C}_\mathrm{R}$ is the constraint weighting matrix and λ is the regularization parameter. The model parameters $\mathbf{m} = [\sigma_1, \sigma_2, h_1]$ are the resistivities σ and thicknesses h of a 2-layered model. The forward response $f(\mathbf{m})$ and its derivatives for the Jacobian matrix are computed using the open-source Python implementation proposed by Werthmüller (2017). The roughening matrix $\mathbf{R}$ applies the lateral constraints as:

$$\mathbf{R}\delta\mathbf{m} = \delta\mathbf{r} + \mathbf{e}_\mathrm{r}, \tag{2}$$

where $\mathbf{e}_\mathrm{r}$ represents the error on the constraints, $\delta\mathbf{r}$ the identity between parameters linked by constraints, and $\delta\mathbf{m} = \mathbf{m} - \mathbf{m}_\mathrm{ref}$. The roughening matrix $\mathbf{R}$ is sparse, containing only diagonals of 1 and -1 for the constrained model parameters (as in Equation 3). Each matrix row enforces a constraint between two model parameters,

$$\mathbf{R} = \begin{bmatrix} 1 & 0 & \dots & 0 & -1 & 0 & \dots & 0 & 0 & 0 \\ 0 & 1 & 0 & \dots & 0 & -1 & 0 & \dots & 0 & 0 \\ \vdots & & & & & \vdots & & & & \vdots \\ 0 & 0 & 0 & \dots & 0 & 1 & 0 & \dots & 0 & -1 \end{bmatrix}. \tag{3}$$

The objective function in Equation 1 is minimized in a Gauss-Newton scheme (executed using the open-source Python method by Rücker et al. (2017)). The model vector $\mathbf{m}$ is updated iteratively following:

$$\mathbf{m}^{k+1} = \mathbf{m}^k + \tau^k \Delta\mathbf{m}^k, \tag{4}$$

using a linear search parameter τ, the superscript k indicates the iteration number. The model update is calculated by:

$$\Delta\mathbf{m}^k = ([\Re[\mathbf{G}^\dagger \mathbf{C}_d \mathbf{G}] + \mathbf{R}\mathbf{C}_m)^{-1} (\Re[\mathbf{G}^T \mathbf{C}_d \delta\mathbf{d}^*] + \lambda \mathbf{R}\mathbf{C}_m \delta\mathbf{m}), \tag{5}$$

where † indicates the complex conjugate transpose and the symbol * indicates complex conjugation.
We propose the following steps to use the information provided by the EMI measurements and to further enhance the results of the ERT inversion:
1. Perform the LCI of EMI measurements.
2. Use the resulting thickness of the first layer as a constraint in the mesh of the ERT inversion.
3. Perform the inversion of ERT measurements using the resulting mesh from the previous step.

Synthetic example

We apply our proposed workflow in a numerical example with two layers, an upper resistive layer and a lower conductive layer (see Subfigure 1a). The simulated EMI and ERT data corresponds to a survey geometry given in Table 1. The results of the LCI of EMI measurements are presented in Subfigure 1b. The estimated model accurately reproduces the conductivities of the two layers and the thickness of the first layer. In Subfigure 1c the results of the ERT inversion are shown. The estimated model from the ERT inversion gradually increases resistivity values with depth, where it is difficult to define a clear boundary between the upper and lower layers. However, it solves very accurately the resistive upper body. In Subfigure 1d the integrated result of ERT inversion using the upper layer thickness from the EMI LCI is presented. The result of this approach shows a better match with the true model and the sharp change in electrical conductivity is more closely reproduced. The ERT data fit improves as well.

Case study

The study area is located on a coastal Dutch polder system in De Cocksdorp, The Netherlands where a level-controlled drainage and subirrigation system has been implemented to retain and better manage

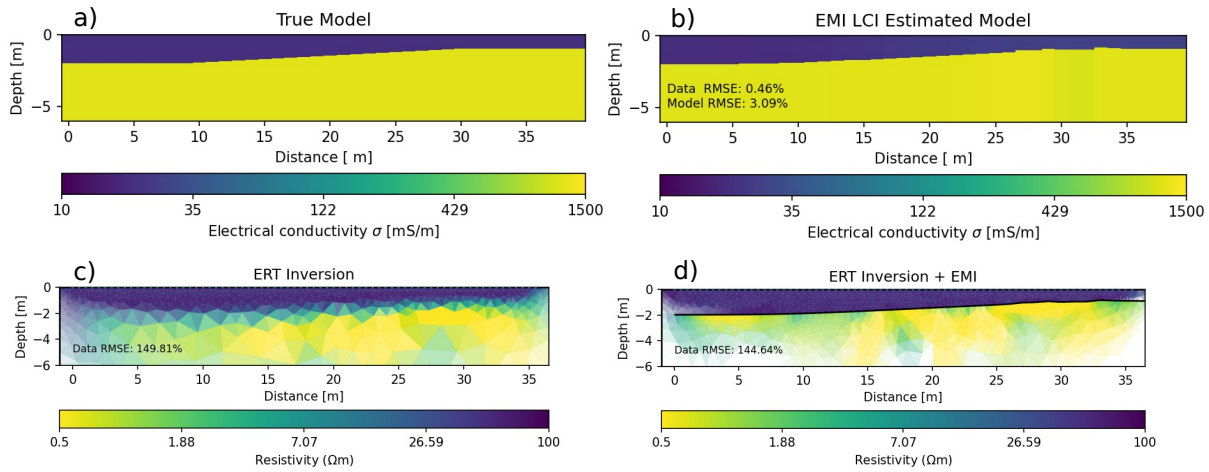

Figure 1 *a) True model, b) 2-layered model estimated using LCI EMI, c) Resistivity model from ERT inversion, d) Resistivity model from ERT inversion using boundary from LCI EMI inversion*

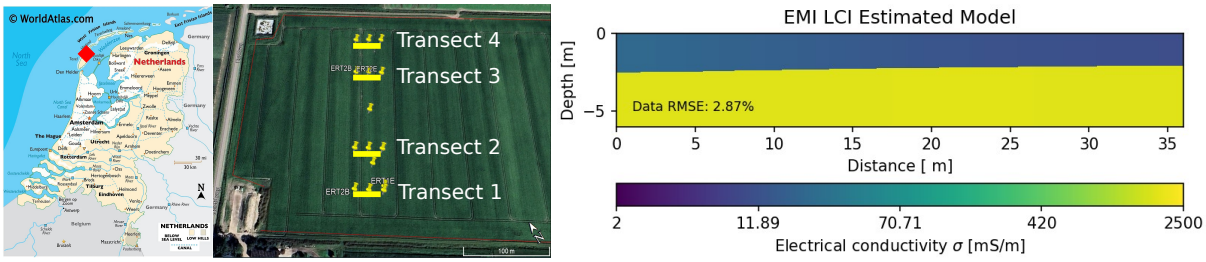

Figure 2 *Left: Area of data acquisition (De Cocksdorp, The Netherlands), Right: EMI LCI estimated 2D model from transect 1*

rainwater. Using the array configurations from Table 1 we acquired 4 transects of EMI and ERT measurements in the area. The results from the EMI LCI in the first transect are shown in Figure 2. The resulting model shows an upper resistive layer presumably containing unsaturated soil or soil saturated with fresher water with an approximate thickness of 3m. The upper layer lies above a lower conductive layer perhaps saturated with brackish/saline water. The ERT corresponding transect is inverted and shown in Figure 3, it presents a smooth transition from a shallow resistive soil to more conductive soil with depth. The thickness of the first layer provided by the EMI LCI estimated model is used as a constraint in the ERT inversion mesh. The resulting ERT + EMI prior information inversion produces a model with a sharper change between the upper resistive and the lower conductive bodies and closer to the estimated EMI LCI conductivity model. The ERT inverted data fit improves when using the constrained mesh. This suggests that using EMI LCI information helps the ERT inversion find a solution closer to the true electrical resistivity distribution of the subsurface.

Conclusions and future work

We investigated the feasibility of using EMI LCI estimated models as prior information in ERT inversion meshes to characterize the changes between an upper resistive soil layer and a lower conductive soil layer. Our methodology was applied to both a synthetic case and a field case study. In the synthetic case, the EMI LCI models are accurately inverted, allowing for better appraisal of the electrical conductivity variations in the ERT inversion. Similarly, in the field case study, incorporating EMI LCI information into the ERT inversion resulted in an estimated model of subsoil resistivity with a sharper delineation of a possible saline groundwater layer, when compared to an ERT inversion without information from EMI measurements. In future work, we aim to acquire repeated EMI and ERT data to assess changes in electrical conductivity over time, influenced by LCD. Additionally, we will measure soil moisture and salinity to evaluate the accuracy of these methods. The approach presented in this study could facilitate

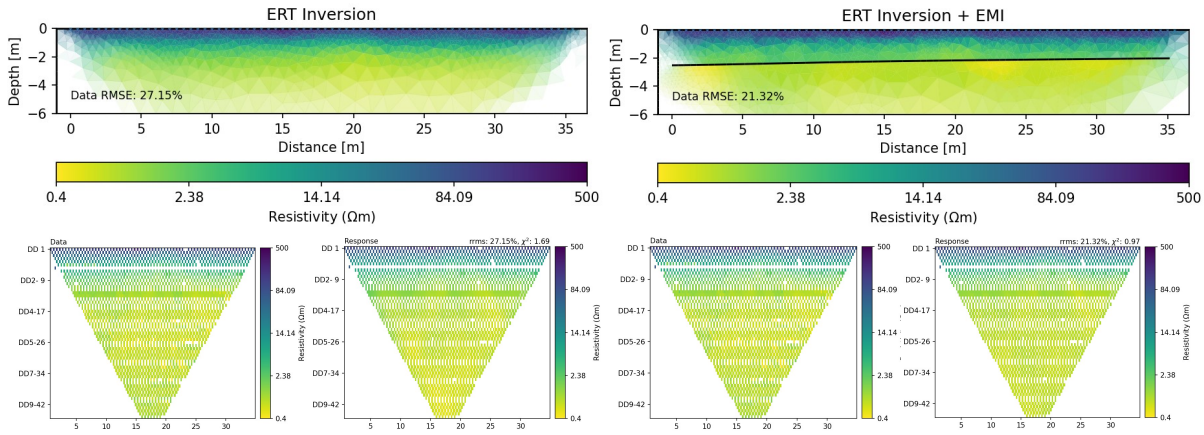

Figure 3 *Top left: ERT inversion results, Top Right: ERT inversion results with EMI boundary in mesh. Bottom left: Data fit from ERT inversion. Bottom right: Data fit from ERT + EMI inversion*

both temporal and spatial monitoring of LCD's impact on RWLs. Furthermore, it could be incorporated into variable-density groundwater numerical models simulating the operation of LCD systems and their impact on the dynamics of RWLs.

Acknowledgments

This publication is part of the project AGRICOAST with project number KICH1.LWV02.20.002 of the research program 'Climate-robust production systems and water management'. AGRICOAST is financially supported by the Netherlands Organization for Scientific Research (NWO), with co-funding from private partner Acacia Water B.V. (acaciawater.com).

References

Auken, E. and Christiansen, A.V. [2004] Layered and laterally constrained 2D inversion of resistivity data. *GEOPHYSICS*, **69**(3), 752–761.

Kearey, P., Brooks, M. and Hill, I. [2002] *An Introduction to Geophysical Exploration*. Geoscience texts. Wiley.

Klose, T., Guillemoteau, J., Vignoli, G. and Tronicke, J. [2022] Laterally constrained inversion (LCI) of multi-configuration EMI data with tunable sharpness. *Journal of Applied Geophysics*, **196**, 104519.

Louw, P.G.B.D., Eeman, S., Essink, G.H.P.O., Vermue, E. and Post, V.E.A. [2013] Rainwater lens dynamics and mixing between infiltrating rainwater and upward saline groundwater seepage beneath a tile-drained agricultural field. *Journal of Hydrology*, **501**, 133–145.

Paepen, M., Hanssens, D., De Smedt, P., Walraevens, K. and Hermans, T. [2020] Combining resistivity and frequency domain electromagnetic methods to investigate submarine groundwater discharge in the littoral zone. *Hydrology and Earth System Sciences*, **24**(7), 3539–3555.

Paz, M.C., Castanheira, N.L., Paz, A.M., Gonçalves, M.C., Monteiro Santos, F. and Farzamian, M. [2024] Comparison of Electromagnetic Induction and Electrical Resistivity Tomography in Assessing Soil Salinity: Insights from Four Plots with Distinct Soil Salinity Levels. *Land*, **13**(3).

Rücker, C., Günther, T. and Wagner, F.M. [2017] pyGIMLi: An open-source library for modelling and inversion in geophysics. *Computers Geosciences*, **109**, 106–123.

Stofberg, S.F., Essink, G.H.P.O., Pauw, P.S., Louw, P.G.B.D., Leijnse, A. and Zee, S.E.A.T.M.V.D. [2017] Fresh Water Lens Persistence and Root Zone Salinization Hazard Under Temperate Climate. *Water Resources Management*, **31**(2), 689–702.

Thalhammer, M.a. [2022] Imaging of active layer characteristics through quasi-3D inversion of frequency-domain electromagnetic soundings.

Werthmüller, D. [2017] An open-source full 3D electromagnetic modeler for 1D VTI media in Python: empymod. *GEOPHYSICS*, **82**(6), WB9–WB19.